Journal of Physiology (1989), **417**, *pp.* 501–518
With 13 *text-figures*
Printed in Great Britain

ELECTRICAL BEHAVIOUR OF MYENTERIC NEURONES IN THE GASTRIC CORPUS OF THE GUINEA-PIG

BY M. SCHEMANN* AND J. D. WOOD

From the Department of Physiology, College of Medicine, The Ohio State University, 4196 Graves Hall, 333 West 10th Avenue, Columbus, OH 43210-1238, USA

(*Received 20 July 1988*)

SUMMARY

1. Electrical behaviour of ganglion cells in the myenteric plexus of the guinea-pig stomach was investigated using intracellular recording methods.

2. Three subpopulations were identified and classified for convenience of discussion as gastric I, II and III neurones. Gastric I neurones were characterized by repetitive spike discharge during depolarizing current pulses and by higher input resistance than the other types. Gastric II neurones discharged one or two spikes only at the onset of long-lasting depolarizing current pulses. Gastric III neurones did not discharge spikes to depolarizing current pulses and had higher membrane potentials and lower input resistances that the other types. Non-stimulus evoked discharge ('spontaneous' discharge) did not occur in any of the neurones.

3. Resting membrane potentials were generated primarily by resting K^+ conductance, but were smaller than the estimated K^+ equilibrium potential. Analysis based on the constant field equation predicted lower K^+ conductance in gastric I than in gastric III neurones.

4. Action potentials in gastric I and II neurones were suppressed or blocked by tetrodotoxin. Spikes that were broadened by tetraethylammonium appeared to have an inward component of Ca^{2+} current.

5. Hyperpolarizing after-potentials were associated with the spikes of both kinds of neurones. These after-potentials had much shorter duration (< 300 ms) than the post-spike hyperpolarization of AH/type 2 intestinal neurones and unlike intestinal neurones there was no latency between the positive after-potential of the spike and the onset of the hyperpolarization. After-hyperpolarization in the gastric neurones was enhanced when the spikes were broadened by tetraethylammonium and was suppressed by removal of Ca^{2+} from the bathing solution.

6. Treatment with either tetraethylammonium or 4-aminopyridine enhanced excitability and induced 'spontaneously' occurring repetitive spike discharge.

7. The electrophysiological behaviour of gastric myenteric neurones differed significantly from intestinal neurones. This was interpreted as specialization of the neural networks that control and co-ordinate the activity of vastly different effector systems in the two regions of the alimentary canal.

* Present address: Institut für Zoophysiologie, Universität Hohenheim, Garbenstrasse 30, D-7000 Stuttgart, FRG.

MS 7130

INTRODUCTION

The enteric nervous system is an independent integrative network that is viewed as a third division of the autonomic nervous system (see reviews by Gershon & Erde, 1981; Wood, 1987*a*). As such, it controls a variety of gastrointestinal functions, including movement of digesta, absorption, regional blood flow and secretory processes including gastric acid secretion and release of hormones. Knowledge of the cellular neurophysiology of enteric ganglion cells of the large and small intestine has increased at an accelerated rate, while no results on electrophysiological behaviour of enteric neurones of the stomach have been reported other than in abstract form (Schemann & Wood, 1987; Schemann, Tamura, Palmer & Wood, 1987). Intracellular electrophysiological studies of vagally innervated parafascicular ganglia near the serosal surface of the opossum stomach have been reported (King & Szurszewski, 1984). Electrical and synaptic activity of these parasympathetic ganglion cells resembled the activity of S/type 1 neurones of the myenteric plexus of guinea-pig small bowel (Nishi & North, 1973; Hirst, Holman & Spence, 1974).

Neurophysiological theory to explain patterns of motor behaviour in the intestine has begun to emerge as new information derived from neurophysiological investigation of the enteric nervous system has been integrated with current concepts of the physiology of the musculature and more precise descriptions of intestinal motor behaviour (Wood, 1987*b*). Patterns of motor behaviour unique to the stomach also appear to be generated by enteric neural mechanisms (Karras, Ren & Schulze-Delrieu, 1987); however, too little is known about the cellular neurophysiology of gastric neurones to permit development of a neurophysiological theory of motor behaviour for the stomach. The stomach represents a highly specialized region of the gastrointestinal tract where it is likely that corresponding specialization of neural control will be reflected by neuronal electrical and synaptic properties different from those in the enteric nervous system of the intestine. The present study was based on this expectation, with the major aim being to determine the electrophysiological behaviour of myenteric neurones of the stomach and compare the results with known properties of intestinal myenteric neurones. The results revealed significant differences between gastric and intestinal neurones that may reflect adaptations for the control of the specialized functions of the stomach.

METHODS

The experimental preparations were obtained from the stomachs of adult male guinea-pigs (250–450 g) after they were stunned by a blow to the head and killed by exsanguination. Immediately after removing the stomach from the animal, a 1·5 cm^2 section was cut from the corpus region and placed in ice-cold Krebs solution in a dissection dish. It was pinned flat under stretch to Sylgard 184 encapsulating resin at the bottom of the dish and the mucosa and inner muscle layers were removed with fine forceps to expose the myenteric plexus on the longitudinal muscle coat. The preparation was then transferred and pinned to Sylgard resin at the bottom of a 1·5 ml recording chamber. This chamber was perfused continuously at 10 ml/min with Krebs–Ringer solution at 36 °C and gassed with 95% O_2–5% CO_2 to buffer at a pH of 7·38. Composition of the Krebs solution (mM) was: NaCl, 120·9; KCl, 5·9; $MgCl_2$, 1·2; NaH_2PO_4, 1·2; $NaHCO_3$, 14·4; $CaCl_2$, 2·5; glucose, 11·5.

Conventional intracellular recording methods with glass microelectrodes filled with 3 M-KCl and having resistances of 100–140 MΩ were used. The individual ganglia were immobilized with L-shaped stainless-steel wires (Wood & Mayer, 1978) and viewed with Nomarski optics using epi-illumination and reflected light as described by Erde, Sherman & Gershon (1985). The preamplifier (Dagan 8100, Dagan Inst., Minneapolis, MN, USA) contained negative capacity compensation and bridge circuitry for injecting electrical current through the microelectrode to control the membrane potential. The amplifier bridge circuit was balanced for each electrode before impalement and balance was adjusted further after impalement by nulling time-independent components of the upstrokes of electrotonic potentials evoked by intraneuronal injection of rectangular pulses of depolarizing current. Electrophysiological data were recorded on videotape and events of interest with slow time courses were replayed for analysis on a strip chart recorder (Gould 2400, Gould Inst., Cleveland, OH, USA). Fast events, including waveforms of action potentials, were recorded and stored by a digital oscilloscope (Hitachi VC6020, Japan) and records were plotted from the digital memory. Time constants for decay of electrotonic potentials and after-potentials associated with spikes were determined as the time required for the potentials to decay to 37% of the initial value.

The fluorescent dye Lucifer Yellow (Steward, 1981) was used to investigate the morphology of the ganglion cells as whole-mount preparations. Microelectrodes were filled with 0·5% Lucifer Yellow (dilithium salt) in 200 mM-$LiCl_2$ and had resistances of 250–300 MΩ. Lucifer Yellow was electrophoresed into the cells with hyperpolarizing current pulses of 0·5–1 s duration and 1 nA for 10–15 min. After allowing 10–15 min for distribution of the dye in the neurone, the preparations were fixed for 2 h in 4% paraformaldehyde in 0·1 M-phosphate buffered solution. A compound microscope (Olympus Vannox) was used for ultraviolet epi-illumination, visualization and photography of the dye-filled neurones.

Karnovski's anticholinesterase stain (Payette, Tennyson, Pham, Mawe, Pomeranz, Rothman & Gershon, 1987) was used to assess the gross morphology of the gastric myenteric plexus of the preparations used in the electrophysiological studies.

Tetrodotoxin (TTX) was dissolved in distilled H_2O. Tetraethylammonium (TEA) was prepared fresh daily as a 1 M stock solution in Krebs solution. 4-Aminopyridine (4-AP) was dissolved in 0·1 M-HCl and the pH adjusted to 7·38 with NaOH. The agents were obtained from Sigma Biochemicals, St Louis, MO, USA. When concentrations of multivalent ions in the bathing solution were altered, normal osmolarity was maintained by appropriate adjustments in the concentration of NaCl.

All values are given as the mean ± standard deviation. A paired t test was used to test for significance of difference in means (Zar, 1974). Probability $< 0·05$ was accepted as significant.

RESULTS

Morphology

The gastric myenteric plexus consisted of ganglia that formed nodes at the intersections of interganglionic fibre tracts (Fig. 1*A*). Each ganglion was estimated to contain ten to fifty ganglion cell somas. Unlike the guinea-pig small intestinal myenteric plexus, which has elongate ganglia oriented in the circumferential axis (Fig. 1*B*), the gastric ganglia were stellate with four to six fibre tracts projecting in all directions away from each ganglion. Impalements were made in ganglion cell bodies located at the nodes of the interganglionic fibre tracts.

Lucifer Yellow injections revealed neuronal-like cells with short processes and a single long process (Fig. 1*D*), cells with two or more long processes (Fig. 1*E*) and cells with broad club-shaped projections and a long process (Fig. 1*C*). The longest of the processes were observed to project through as many as three rows of ganglia. Processes of all the cells were generally smooth but some had regions with multiple varicosities, especially within the ganglia.

Electrical behaviour

The results were obtained from successful impalements in 187 neurones in preparations from 100 guinea-pigs. Impalements were judged successful if the resting membrane potential was stable and in excess of −40 mV, if the action potentials

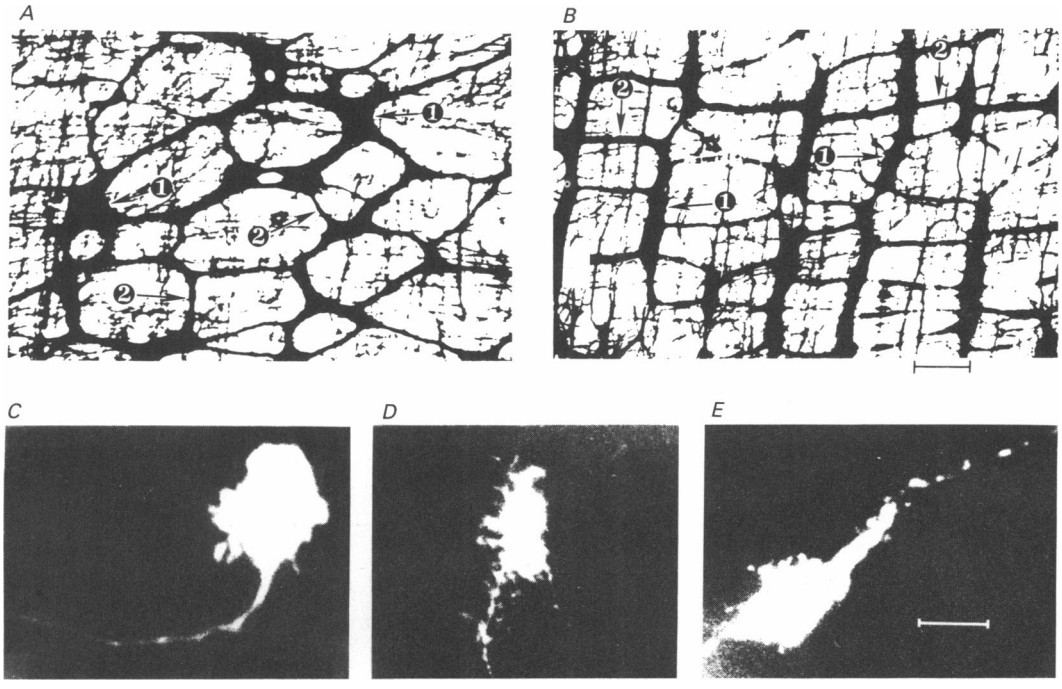

Fig. 1. Comparative morphology of the gastric myenteric plexus of the guinea-pig. *A*, myenteric plexus of the gastric corpus stained for acetylcholinesterase. Primary plexus consists of stellate-shaped ganglia at the nodes of interganglionic fibre tracts. A secondary plexus of cholinesterase positive fibres underlies the primary plexus on the longitudinal muscle. *B*, myenteric plexus of the guinea-pig jejunum stained for acetylcholinesterase. Primary plexus consists of fusiform ganglia oriented in the circumferential axis and connected by interganglionic fibre tracts. A secondary plexus of cholinesterase-positive fibres underlies the primary plexus on the longitudinal muscle. *C–E*, individual ganglion cells in the gastric myenteric plexus filled with the fluorescent dye Lucifer Yellow. Calibration bar for *A* and *B*, 200 μm; for *C–E*, 20 μm.

depolarized beyond zero membrane potential and if the impaled neurone showed no swelling during the course of the impalement.

Three types of neurones were distinguished based on distinctive electrophysiological behaviour that never changed throughout impalements lasting from 10 min to 5 h. For convenience of discussion, these are referred to as gastric I, II and III myenteric neurones. Gastric I neurones comprised 47·6% of the impaled neurones, gastric II neurones made up 33·7% and gastric III neurones made up 18·7%.

None of the neurones displayed any fluctuations of membrane potential that could be interpreted as pacemaker activity and none discharged spikes spontaneously.

Gastric I neurones were the most excitable of the three types. This was

distinguished by repetitive discharge of action potentials in response to intrasomatic injection of 100–200 ms duration depolarizing current pulses (Fig. 2). The frequency of discharge increased in direct relation to the strength of the injected pulse and discharge occurred throughout stronger pulses (Fig. 2*C* and *D*). Maximum rate of

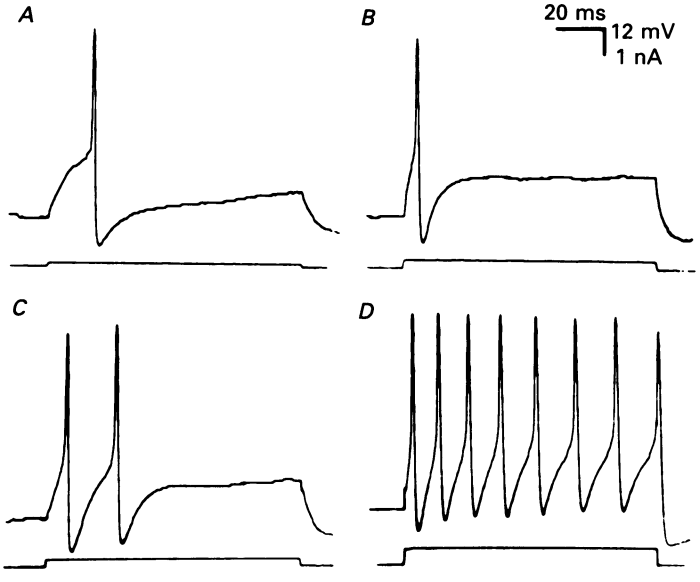

Fig. 2. Electrophysiological behaviour of a gastric I and II neurones in the guinea-pig myenteric plexus. *A*, gastric II neurone discharged a single spike at the onset of a depolarizing current pulse. *B*, same gastric II neurone did not fire repetitively to depolarizing current of increased strength. *C*, gastric I neurone discharged two spikes at the onset of a depolarizing current pulse. *D*, same gastric I neurone discharged repetitively throughout a depolarizing current pulse of increased strength. Resting potential of gastric I cell was −54 mV; gastric II −55 mV.

discharge during the strongest pulses was 100 Hz. The neurones did not discharge repetitively throughout longer duration depolarizations. In fifteen neurones that were depolarized with supramaximal current for 1 min, ten to fourteen action potentials were fired at the beginning of the pulse, after which discharge stopped for the remainder of the depolarization. Recovery of repetitive discharge to the next depolarizing pulse occurred within 2 s.

Interspike intervals progressively increased during the repetitive discharge and the rates of rise and fall of the action potential (dV/dT) decreased (Fig. 2). The greatest change in dV/dT occurred for the rising phase of the spike. For nine neurones at the maximal rate of discharge during a 100 ms pulse, the mean dV/dT for the rising phase of the last spike was $67{\cdot}4 \pm 9{\cdot}5\%$ of the first spike, while the dV/dT of the falling phase of the last spike was $79{\cdot}7 \pm 8{\cdot}9\%$ of the first spike. The mean value of the maximal dV/dT of the upstroke of the action potential was 98 ± 20 V/s and the value for the downstroke was 75 ± 16 V/s.

The mean resting potential for eighty-nine gastric I neurones was $-58{\cdot}6 \pm 7{\cdot}6$ mV. Threshold for spike discharge was $-38{\cdot}7 \pm 9{\cdot}8$ mV. Anodal-break excitation at the offset of hyperpolarizing current pulses of any strength was not a consistent

characteristic of the gastric I neurones. The electrotonic potential at the offset of hyperpolarizing current pulses decayed exponentially with a time constant of 4·1 ± 0·8 ms. Gastric I neurones had a mean input resistance of 155 ± 71 MΩ as determined from the slopes of current–voltage plots. Current–voltage relations for hyperpolarizing current were ohmic for current strengths less than 400 pA (Fig. 3). Marked rectification occurred with larger hyperpolarizing pulses and with depolarizations from the resting potential (Fig. 4).

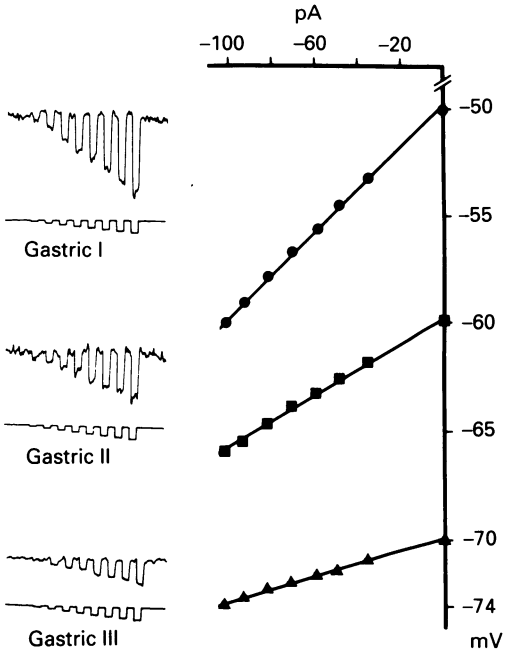

Fig. 3. Comparison of current–voltage relations for types I, II and III gastric myenteric neurones. Records on left show programmed sequence of eight constant current pulses that was injected into each neuronal cell body. Bottom traces show current; upper traces show electrotonic potentials produced by current pulses. Current–voltage curves were plotted as change in membrane potential during each electrotonic potential on the vertical axis *vs.* strength of current pulses on horizontal axis. Incremental decreases in the slopes of the curves from gastric I to gastric III neurones reflect ordered decreases in input resistance for each of the cell types. Input resistance was 119 MΩ for the gastric I neurone, 74 MΩ for the gastric II, and 33 MΩ for the gastric III neurone.

Gastric II neurones usually discharged a single action potential at the onset of depolarizing current pulses (Fig. 2). Two spikes sometimes occurred in response to high-intensity pulses, but this was rare. Repetitive discharge, as observed in gastric I cells, never occurred during pulses of any strength or duration. Threshold for spike discharge was −31·1 ± 10·2 mV which was significantly more depolarized than for gastric I neurones.

Mean resting potential for sixty-three gastric II neurones was −59·6 ± 7·3 mV and was not significantly different from gastric I cells. The mean input resistance of 85·2 ± 35·3 MΩ was significantly lower than for gastric I neurones (Fig. 3). Five of the gastric II neurones showed anodal-break excitation at the offset of hyperpolarizing

pulses. The electronic potentials at the offset of hyperpolarizing current pulses decayed exponentially with a time constant of $2{\cdot}0 \pm 0{\cdot}8$ ms. The dV/dT values for the rising and falling phases of the spike were 93 ± 20 and 71 ± 14 V/s respectively, which were comparable with these parameters for gastric I cells.

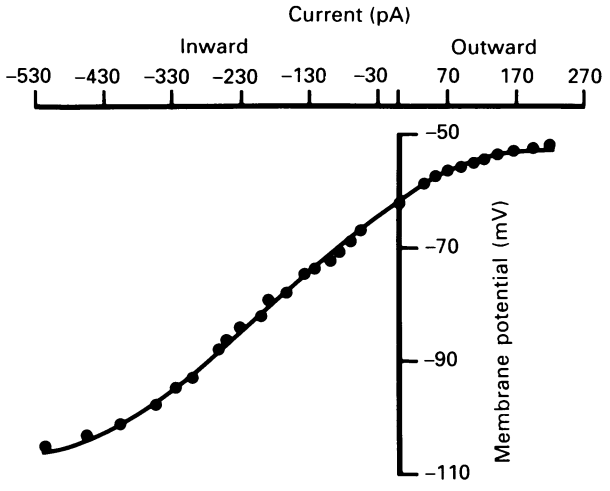

Fig. 4. Current–voltage relation for a gastric II neurone shows an ohmic segment flanked by evidence of rectification at the depolarized and hyperpolarized portions of the curve.

Gastric III neurones never discharged action potentials in response to depolarizing current pulses irrespective of the strength of the injected current, even for currents that depolarized beyond zero membrane potential. These were identified as neurones on the basis of stimulus-evoked synaptic potentials (Schemann & Wood, 1987), and in some of the cells, discharge of a few spikes upon impalement.

Mean resting potential of thirty-five gastric III neurones was $-67{\cdot}7 \pm 7{\cdot}7$ mV which was significantly greater than that of the other two neuronal types. The mean input resistance of $41 \pm 16{\cdot}4$ MΩ was significantly lower than that for the other neurones (Fig. 3), as was the membrane time constant of $1{\cdot}1 \pm 0{\cdot}5$ ms.

Resting potentials

Elevation of the K^+ concentration in the bathing medium depolarized the membrane potential (Fig. 5). The relation between the logarithm of K^+ concentration and membrane potential was predicted by the Goldman–Hodgkin–Katz constant field equation (Fig. 5). The membrane potentials of gastric I neurones were more depolarized than gastric III neurones over a range of external K^+ concentrations between 1 and 20 mM (Fig. 5). Permeability ratios required to fit the data to values predicted by the constant field equation are given in Fig. 5. In order to fit the data for gastric I neurones, a value of 35 for K^+ permeability was used in the equation, whereas a K^+ permeability of 150 was required to fit the data for gastric III neurones. This is consistent with a significantly higher resting K^+ conductance for gastric III neurones and probably accounts for lower input resistances in these cells relative to the gastric I neurones.

Action potentials

The amplitudes of the action potentials in both gastric I and gastric II neurones ranged from 60 to 110 mV. Duration of the spikes determined at half the maximal amplitude was $1{\cdot}2 \pm 0{\cdot}1$ ms. There was no broadening of the falling phase of the

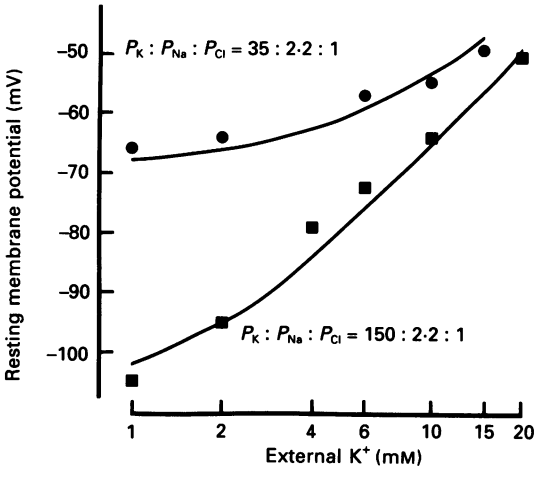

Fig. 5. Relation between membrane potential and logarithm of K^+ concentration in the bathing medium for gastric I (●) and gastric III (■) neurones. The points on the curves are measured values. The curves were fitted to the data points with the Goldman–Hodgkin–Katz constant field equation. The following intracellular ion concentrations (mM) were inserted into the constant field equation: $K^+ = 140$; $Na^+ = 10$; $Cl^- = 10$. The permeability ratios used for plotting the curve for each neurone are given.

action potentials comparable to that of AH/type 2 intestinal neurones (Wood & Mayer, 1978). In intestinal AH/type 2 neurones, the 'shoulder' on the falling phase of the spike is apparent as decreased slope on records of dV/dT (Fig. 6). No aberration of this nature was associated with the spikes of the gastric neurones. Unlike AH/type 2 neurones, the rate of repolarization of the membrane potential accelerated uniformly with time.

Hyperpolarizing after-potentials

Hyperpolarizing after-potentials, of short duration relative to the after-hyperpolarization of intestinal AH/type 2 neurones (Nishi & North, 1973; Hirst *et al.* 1974), were associated with the action potentials of both gastric I and II neurones (Figs 7 and 10). Unlike the long-lasting after-hyperpolarization of AH/type 2 neurones which is delayed 45–80 ms after the positive after-potential of the spike (Wood & Mayer, 1978), the after-hyperpolarization of gastric neurones was continuous with the negative undershoot of the spike.

The amplitude of the after-hyperpolarization ranged from 5 to 15 mV and the duration ranged from 10 to 270 ms. Time constants for the decay of the after-potentials ranged between 19 and 112 ms. The amplitude of the after-hyperpolarization of gastric I neurones did not increase with the number of spikes

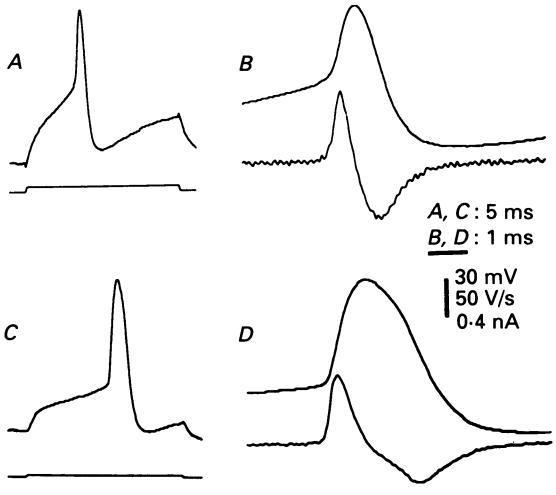

Fig. 6. Comparative waveforms of the action potentials of neurones in the myenteric plexus of the guinea-pig stomach and small intestine. *A*, action potential evoked in a gastric II neurone by intrasomatic current injection. *B*, same action potential as in *A* recorded with an expanded time base and with dV/dT on the bottom trace. *C*, action potential evoked in an AH/type 2 intestinal neurone by intrasomatic current injection. *D*, same action potential as in *C* recorded with an expanded time base and with dV/dT on the bottom trace. Broadened spike and decreased dV/dT is characteristic of intestinal but not gastric neurones. Resting potential of gastric II neurone was −80 mV and the resting potential of the AH/type 2 neurone was −79 mV.

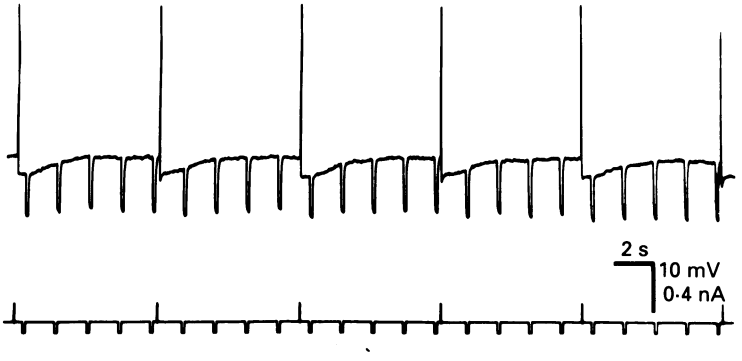

Fig. 7. Hyperpolarizing after-potentials in a gastric II neurone were associated with decreased input resistance. Action potentials were evoked by depolarizing current pulses shown on bottom trace. Hyperpolarizing electrotonic potentials were produced by repetitive injection of constant pulses of outward current. Reduced amplitude of electrotonic potentials during the post-spike hyperpolarization reflect a decrease in the input resistance. The after-hyperpolarization was exaggerated by treatment with 10 mM-TEA. There was TTX (1 μM) present throughout the experiment. Resting potential was −70 mV.

discharged repetitively during depolarizing pulses of constant amplitude and progressively increasing duration (Fig. 8). The amplitude of the hyperpolarization did increase if spike frequency was increased by increasing the amplitude of constant duration depolarizing pulses. This occurred whether or not spike discharge was evoked by the pulses. During spike blockade in TTX, depolarizing current pulses of any duration were followed by membrane hyperpolarization. The hyperpolarization in this case increased in amplitude and duration with increased amplitude of the current pulses.

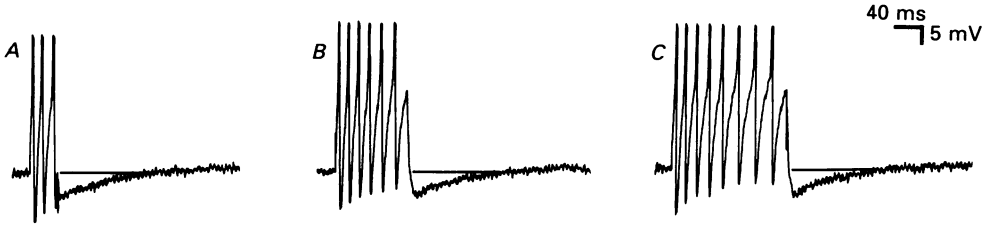

Fig. 8. Hyperpolarizing after-potentials in a gastric I neurone. *A*, hyperpolarization following discharge of three action potentials. *B*, increased duration of current pulse from 40 to 90 ms increased number of spikes to 6 without change in after-hyperpolarization. *C*, increased duration of current pulse from 90 to 150 ms evoked 8 spikes without change in after-hyperpolarization. Amplitude of current pulses was constant throughout. Full amplitude of spikes is off scale.

The relative refractory period for evoking single spikes with short-duration depolarizing pulses (< 10 ms) was prolonged by the post-spike hyperpolarization.

Electrotonic potentials produced by intrasomatic injection of constant-current (duration < 20 ms) hyperpolarizing pulses were reduced in amplitude during the hyperpolarizing after-potentials (Fig. 7). This was indicative of a decrease in the input resistance of the cell during the after-hyperpolarization.

In seven gastric I neurones, the amplitude of the after-hyperpolarization was reduced when the membrane potential was current clamped to progressively greater levels of hyperpolarization and no hyperpolarization occurred at membrane potentials of about -90 mV. This suggested that the reversal potential was near -90 mV, which is close to the equilibration potential for K^+.

Additional evidence for increased K^+ conductance was reduction in the amplitude of the hyperpolarizing response in direct proportion to increase in the concentration of the K^+ in the bathing medium and in parallel with decreases in the membrane potential (Fig. 9). The reversal potential for the hyperpolarizing responses occurred at progressively lower membrane potentials as external K^+ was increased and this relation followed reductions in the K^+ equilibrium potential as predicted by Nernstian theory (Fig. 9).

Treatment with TEA (10 mM) prolonged the hyperpolarizing response coincident with broadening of the action potential (Fig. 10*C*). Removal of Ca^{2+} from the bathing medium resulted in marked suppression of the hyperpolarizing response (Fig. 10*D*). In addition, removal of Ca^{2+} from the bathing medium containing 10 mM-TEA also resulted in marked suppression of the hyperpolarizing response. Treatment with

4-AP reduced the amplitude and duration of the hyperpolarizing after-potentials without measurable effects on the shape of the action potentials (Fig. 10*B*).

Effects of tetrodotoxin, tetraethylammonium and 4-aminopyridine

The action potentials of all thirty gastric I and sixteen gastric II neurones were either suppressed or abolished by TTX. Application of 0·1 μM-TTX in the superfusion

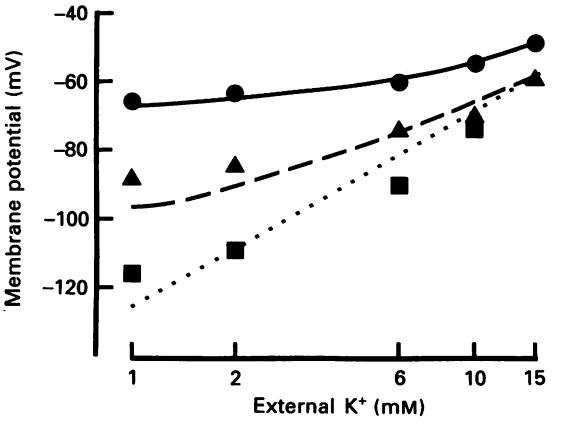

Fig. 9. Relations between membrane potential, characteristics of post-spike hyperpolarizing potentials and the concentration of K^+ in the external bathing medium for a gastric II neurone. ●, data for effects of altered external K^+ on resting membrane potential; ▲---▲, changes in the maximal amplitude of the after-hyperpolarization relative to external K^+; ■ (no connecting line), relation between the measured reversal potential of the after-hyperpolarization and the external K^+; ····· (no data points), theoretical relation between the membrane potential and the given values of external K^+ as calculated from the Nernst equation using a value of 140 mM for intracellular K^+.

solution always abolished spikes evoked by injected current at or near threshold strength for spike discharge (Fig. 11*B*). When this occurred, large increases in the strength of the depolarizing current evoked oscillations of membrane potential resembling aborted spikes in gastric I neurones (Fig. 11*B*) and a single small abortive spike at the onset of the current pulse in gastric II cells. These aborted spikes in both types of neurones persisted for up to 30 min in the presence of TTX. The effects of TTX were reversed within 10–30 min after wash-out of the drug.

Application of 10 mM-TEA in the presence of TTX restored spike amplitude to nearly the same or a greater level than before TTX (Fig. 11*C*). These spikes were broadened by a pronounced 'shoulder' on the falling phase of the spike. Removal of Ca^{2+} from the bathing solution or addition of 2·5 mM-Co^{2+} abolished the broadened spikes in the presence of TTX and TEA (Fig. 11*D*). The spikes returned to normal within 15–30 min of return to superfusion with normal Krebs solution.

The spikes were broadened in sixteen neurones after addition of 10 mM-TEA to the superfusion solution without TTX (Fig. 12*B*). This resulted in an increase of 10–50 ms in the duration of the spike at half-maximal amplitude that was due to prolongation of the repolarization phase of the spike. The 'shoulder' on the falling

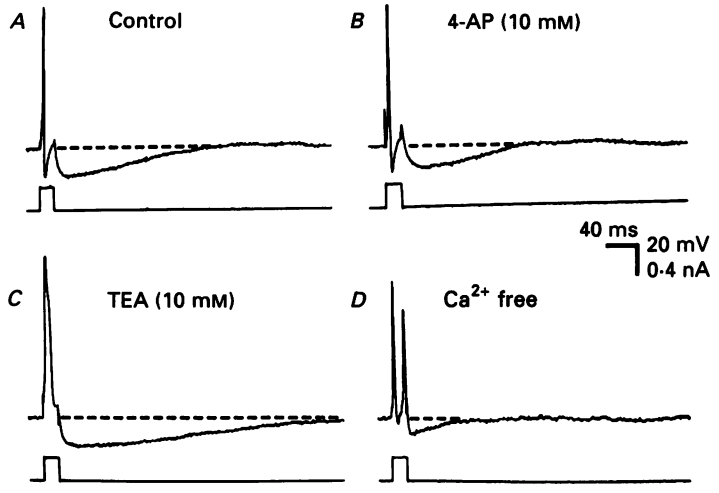

Fig. 10. Effects of TEA, 4-AP and removal of Ca^{2+} on hyperpolarizing after-potentials in gastric II neurone. *A*, control response. *B*, treatment with 4-AP shortened the after-hyperpolarization. *C*, treatment with TEA prolonged the after-hyperpolarization. *D*, removal of Ca^{2+} from the bathing medium suppressed the post-spike hyperpolarization. Resting potential was −63 mV and was clamped at this potential throughout the experiment.

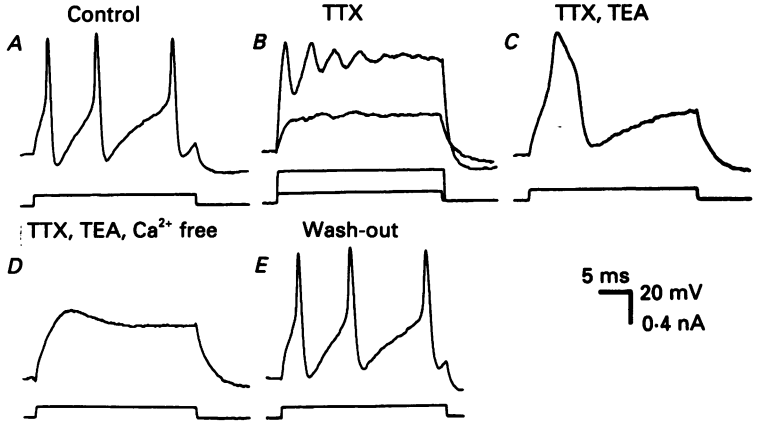

Fig. 11. Effects of TTX, TEA and reduced Ca^{2+} on electrophysiological behaviour of a gastric I neurone. *A*, control response consisted of repetitive spike discharge to a depolarizing current pulse. *B*, application of 1 μM-TTX blocked spike discharge to pulses of control strength. Increase in the current strength (superimposed trace) evoked 'aborted' spikes in TTX. *C*, application of 10 mM-TEA restored the spike to pulses of control amplitude in the continued presence of TTX. The spikes in TTX and TEA were broadened with a pronounced 'shoulder'. *D*, no spikes were evoked by any strength of depolarizing current after removal of Ca^{2+} from the bathing medium containing TTX and TEA. *E*, the neurone returned to control behaviour after washing out the TTX and TEA and replacing the Ca^{2+}. Resting potential was −53 mV.

phase of the spike in TEA appeared as a region of decreased slope on records of dV/dT. In addition to broadening the spike, treatment with TEA also increased the amplitude of the action potentials by 10–20% of the control (Fig. 12*D*). This occurred coincidentally with increase in spike-associated hyperpolarizing after-potentials and a decrease in the negative undershoot of the spike.

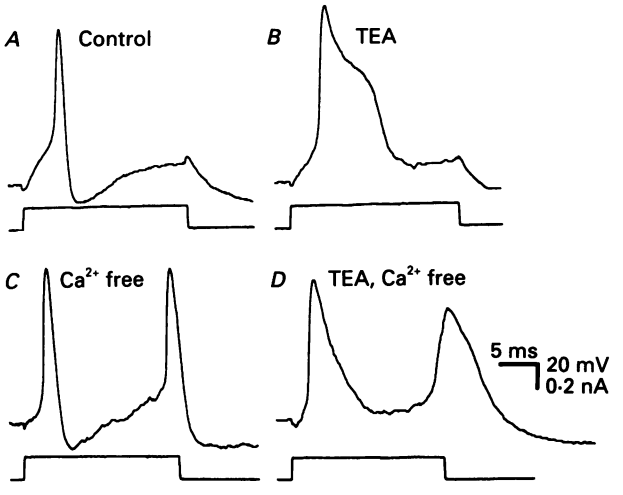

Fig. 12. Effects of TEA and reduced Ca^{2+} on electrophysiological behaviour of a gastric I neurone. *A*, control response consisted of a single spike to a depolarizing current pulse. *B*, application of 10 mM-TEA resulted in a broadened spike with pronounced 'shoulder' on the repolarization phase. *C*, removal of Ca^{2+} from the bathing medium in the absence of TEA increased excitability as reflected by multiple spikes to depolarizing current pulses. *D*, removal of Ca^{2+} in the presence of TEA resulted in narrowing of the spike due to suppression of the 'shoulder' on the repolarization phase of the spike. Resting potential was −64 mV and was clamped at this level throughout the experiment.

Removal of Ca^{2+} from the bathing solution containing TEA resulted in partial reversal of the effects of TEA on the spikes. Within 2–5 min of removing the Ca^{2+}, the spike duration was shortened and the amplitude was significantly reduced (Fig. 12*D*).

Application of TEA or 4-AP (10 or 20 mM) increased the excitability of gastric I and II neurones (Fig. 13). Enhanced excitability was apparent as appearance of spontaneous spike discharge in association with membrane depolarization and increased input resistance, and as increased spike discharge during depolarizing current pulses. After TEA, but not 4-AP, hyperpolarizing after-potentials appeared and became progressively larger in amplitude and longer in duration as the frequency of spike discharge increased (Fig. 13*B*). Enhancement of the hyperpolarizing after-potentials occurred simultaneously with broadening of the action potentials in TEA. These actions of TEA and 4-AP were reversed 5–10 min after removal of the substances from the superfusion solution. Neither TEA nor 4-AP induced spike discharge in gastric III neurones.

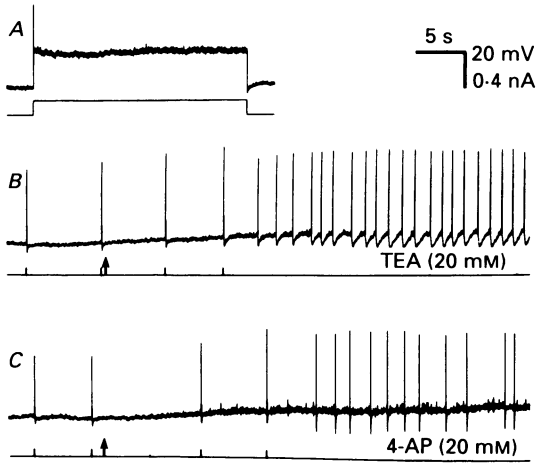

Fig. 13. TEA or 4-AP evoked spontaneous spike discharge in a gastric II neurone. *A*, a long-lasting depolarizing current pulse evoked a single spike in the absence of drugs. *B*, application of 20 mM-TEA (arrow) resulted in spontaneous spike discharge with concomitant increase in the hyperpolarizing after-potentials associated with the spikes. *C*, application of 20 mM-4-AP (arrow) resulted in spontaneous spike discharge. Unlike TEA, there was no enhancement of post-spike hyperpolarizing potentials. The first four spikes in the records of *A* and *B* were evoked by the depolarizing current pulses shown on the bottom trace of each record. Resting potential was −48 mV.

DISCUSSION

Comparative characteristics of gastric neurones

This appears to be the first study of electrophysiological behaviour of ganglion cells in the myenteric plexus of the stomach. The results of the study revealed similarities to the behaviour of enteric ganglion cells of the intestine, as well as considerable differences. Gastric neurones were like intestinal neurones in that subpopulations with common behavioural characteristics were observed. Three subpopulations were characterized and referred to as gastric types I, II and III neurones. These subpopulations each had properties that differed from those of the subgroups of intestinal neurones (see Wood, 1987*a*, 1989 for reviews of the classification and properties of enteric neurones of the intestine).

Gastric I neurones were like intestinal S/type 1 neurones in that they had higher input resistances and longer membrane time constants than neurones in the other subgroups. These neurones discharged repetitively during depolarizing current pulses and in this respect resembled S/type 1 intestinal neurones. The repetitive discharge of gastric I neurones did not continue during sustained depolarization and differed from S/type 1 neurones which continue to discharge repetitively during long-lasting depolarization. Infrequent occurrence of anodal-break excitation at the offset of hyperpolarization in the gastric I cells also distinguished them from S/type 1 neurones.

Gastric II neurones were like intestinal AH/type 2 neurones in that they were less excitable than gastric I neurones, as revealed by discharge of only one or two spikes

at the onset of depolarizing current pulses. Input resistances and membrane time constants of the gastric II cells were less than the more excitable gastric neurones, which is also a characteristic of AH/type 2 neurones in the intestine.

A major difference between the gastric II neurones and AH/type 2 intestinal neurones was the absence of long-lasting hyperpolarizing after-potentials in the neurones of the stomach. The after-hyperpolarization of AH/type 2 intestinal neurones begins 40–100 ms after termination of the positive after-potential of the spike and has a time course of several seconds. No hyperpolarizing after-potentials with these properties were ever observed in the gastric neurones. Spikes in the gastric II neurones were followed by hyperpolarizing after-potentials; however, these were never delayed after the positive after-potential and were never longer than 270 ms.

Gastric III neurones never discharged spikes to depolarizing current injection and were reminiscent of type 3 intestinal neurones in this respect. These cells in the stomach appeared to be neurones based on the presence of nicotinic cholinergic synaptic inputs and in some cases on initial spike discharge upon impalement. Like intestinal type 3 neurones, they were distinguished by high resting potentials, low input resistance and short membrane time constants. Lucifer Yellow injections in a few cells revealed morphological characteristics of neurones. Nevertheless, not all of these criteria for identification as neurones were met in all of the inexcitable cells and the possibility that some were glial cells cannot be ruled out.

The somatic membranes of the type 3 neurones in the intestine behave like dormant neurones that receive fast synaptic inputs, but are inexcitable in terms of action potential generation. Stimulation of adenylate cyclase in these cells activates spike discharge (Wood, 1987*c*). This aspect of gastric III neurones has not been fully explored and the existence of similar behaviour in these neurones is uncertain.

Resting potentials

The resting membrane potentials of the gastric neurones were primarily K^+ equilibrium potentials and in this respect were the same as other enteric neurones. This was evidenced by a good fit to the Goldman–Hodgkin–Katz constant field equation of experimental data on relations between external K^+ and the membrane potential. Analysis of these data with the constant field equation suggested that the resting K^+ conductance was lowest in the gastric I neurones and that this accounted for the higher input resistance recorded in these cells. This would be expected to result also in lower values for the resting membrane potential in the gastric I cells. There was a tendency for this to be the case; however, interneuronal variability was sufficiently high that the differences were not statistically significant.

The equilibrium potential for K^+ is predicted to be in the range of -80 to -90 mV for all enteric neurones (see North, 1986; Wood, 1987*a*, 1989). Reversal potentials in this range for membrane events involving putative K^+ channels suggest that this is the situation also for the gastric neurones. Values for the resting membrane potentials in gastric neurones, as well as other enteric neurones, are substantially less than the K^+ equilibrium potential. This provides a mechanism whereby receptor-mediated opening or closure of K^+ channels can modulate membrane potential in the hyperpolarizing or depolarizing direction. In other enteric neurones, these changes in membrane potential are recognized as slow inhibitory or

slow excitatory postsynaptic potentials, respectively, (see North, 1986; Wood, 1987*a*, 1989). Resting membrane potentials less than the K^+ equilibrium potential in gastric neurones would permit this kind of neuromodulation; nevertheless, our studies of synaptic behaviour have not revealed significant occurrence of slow synaptic potentials in the gastric neurones (Schemann & Wood, 1987).

Action potentials

Sensitivity of the action potentials of both types of gastric neurones to TTX suggest a strong contribution of Na^+ channels to the inward currents of the spikes. This is similar to S/type 1 neurones of the intestine, but unlike AH/type 2 intestinal neurones. The AH/type 2 intestinal neurones often have a 'shoulder' on the falling phase of the action potential indicative of a significant inward Ca^{2+} current during the spike (Hirst & McKirdy, 1973, Hirst, Johnson & van Helden, 1985). There was no broadening of the spike in the gastric neurones that would suggest a Ca^{2+} component.

Treatment of gastric neurones with TEA broadened the spikes, presumably as a result of blockade of the time- and voltage- dependent K^+ channels responsible for the repolarization phase. The 'shoulders' that appeared at the falling phase of the spikes in TEA seemed to reflect the opening of Ca^{2+} channels, because they were suppressed by reduction of Ca^{2+} in the extracellular medium. Limitations of our recording methods make this a tentative interpretation; nevertheless, the results are consistent with time- and voltage-sensitive Ca^{2+} channels being present in the somatic membranes of the gastric neurones. On the other hand, the functional significance of these channels is questionable because they seem to require blockade of some of the delayed rectifier current and consequent delay in repolarization in order for them to 'turn on'.

Treatment with TEA or 4-AP resulted in the appearance of spontaneous repetitive spike discharge in types I and II gastric neurones. These neurones never showed non-stimulus-evoked discharge in the absence of these agents. Again, the limitations of our methods for assessment of individual channel currents make interpretation of these results tentative. Nevertheless, they suggest that the relatively low excitability of the neurones under the normal conditions of the experiment result from operation of K^+ conductances that are suppressed by TEA or 4-AP. The action of TEA, which enhanced the hyperpolarizing after-potentials and broadened the spikes, was probably the result of blockade of conductance in delayed rectifier channels. Either TEA or 4-AP enhanced neuronal excitability, resulting in repetitive discharge. This effect may have been due to blockade of A-currents by 4-AP or TEA. Unlike TEA, 4-AP did not enhance the hyperpolarizing after-potentials, suggesting lack of action of 4-AP on the delayed rectifier currents.

Hyperpolarizing after-potentials

Like the after-hyperpolarization of intestinal AH/type 2 neurones, the post-spike hyperpolarization of the gastric neurones lengthened the relative refractory period of the action potential. This occurred in a time domain of milliseconds for the gastric neurones, whereas the relative refractory period of AH/type 2 neurones is prolonged

by several seconds. Relative to post-spike hyperpolarizing potentials, the neurones of the gastric myenteric plexus in the guinea-pig differed from the large parafascicular ganglia on efferent paths to the opossum stomach. No hyperpolarizing after-potentials were reported for the opossum neurones which were described as behaving like S/type 1 neurones of the guinea-pig intestinal myenteric plexus (King & Szurszewski, 1984).

Unlike AH/type 2 intestinal neurones, the after-hyperpolarization in gastric neurones did not summate with discharge of increased numbers of action potentials. When the number of spikes was increased by prolonged duration of constant amplitude current pulses, there was no change in the after-spike hyperpolarization in the gastric neurones. On the contrary, increased amplitude of depolarizing current pulses did lead to increased amplitude and duration of the after-hyperpolarization. This occurred also in the absence of spike discharge, suggesting that depolarization *per se* accounts for the hyperpolarization following offset of the current pulse.

The ionic mechanism for the after-hyperpolarization in the gastric neurones appeared to be an increase in K^+ conductance. Evidence for this was decreased input resistance, a reversal potential near the estimated K^+ equilibrium potential and reduction in amplitude in proportion to reduction of the K^+ concentration gradient across the membrane. Increased K^+ conductance is also the accepted mechanism for the hyperpolarizing after-potentials in AH/type 2 intestinal neurones. In AH/type 2 neurones, a characteristic 'shoulder' on the falling phase of the action potential is thought to reflect inward Ca^{2+} current which is a trigger for opening of Ca^{2+}-dependent K^+ channels and production of post-spike hyperpolarization. No 'shoulders' were associated with the spikes of the gastric neurones, although evidence for a mechanism involving Ca^{2+}-dependent K^+ conductance increase was obtained. The hyperpolarizing after-potentials in the gastric neurones were enhanced coincidentally with broadening of the spikes by TEA. Removal of Ca^{2+} from the bathing solution reversed this effect on the after-hyperpolarization, suggesting that the enhanced after-potentials resulted from augmented influx of Ca^{2+} during the broadened spikes in TEA.

Conclusions

The results of this study revealed pronounced differences in the details of the electrophysiological behaviour of intramural ganglion cells of the stomach as compared with the intestine of the guinea-pig. This was not unexpected because the neural networks of the stomach must control and co-ordinate behaviour of motor and secretory effector systems that is entirely different from the intestine. Consequently, it would be surprising if neurophysiological specialization were not found in the gastric division of the enteric nervous system. The following paper (Schemann & Wood, 1989) describes specialization of synaptic interactions that underscore the differences in the neural correlates of behaviour of the stomach and intestine.

This research was supported by National Institutes of Health Grant 5 R01 DK37238 to J. D. W. and Deutsche Forschungsgemeinschaft Fellowship Sche 267/1-1 and 267/1-2 to M.S.

REFERENCES

ERDE, S. M., SHERMAN, D. & GERSHON, M. D. (1985). *Journal of Neuroscience* **5**, 617–633.

GERSHON, M. D. & ERDE, S. M. (1981). The nervous system of the gut. *Gastroenterology* **80**, 1571–1594.

HIRST, G. D. S., HOLMAN, M. E. & SPENCE, I. (1974). Two types of neurones in the myenteric plexus of duodenum in the guinea-pig. *Journal of Physiology* **236**, 303–326.

HIRST, G. D. S., JOHNSON, S. M. & VAN HELDEN, D. F. (1985). The calcium current in a myenteric neurone of the guinea-pig ileum. *Journal of Physiology* **361**, 297–314.

HIRST, G. D. S. & MCKIRDY, H. C. (1973). Calcium action potentials in mammalian peripheral neurones. *Nature* **243**, 54–56.

KARRAS, P., REN, J. & SCHULTZE-DELRIEU, K. (1987). Spread of nerve mediated responses through the isolated cat stomach. *Gastroenterology* **92**, 1460.

KING, B. F. & SZURSZEWSKI, J. H. (1984). Intracellular recordings from vagally innervated intramural neurons in opossum stomach. *American Journal of Physiology* **9**, G209–212.

NISHI, S., NORTH, R. A. (1973). Intracellular recording from the myenteric plexus of the guinea-pig ileum. *Journal of Physiology* **231**, 471–491.

NORTH, R. A. (1986). Mechanisms of autonomic integration. In *Handbook of Physiology*, sect. 1, vol. IV, ed. BLOOM, F. E., pp. 115–153. Bethesda, MD, USA: American Physiological Society.

PAYETTE, R. F., TENNYSON, V. M., PHAM, T. D., MAWE, G. M., POMERANZ, H. D., ROTHMAN, T. P. & GERSHON, M. D. (1987). Origin and morphology of nerve fibers in the aganglionic colon of the lethal spotted (*ls/ls*) mutant mouse. *Journal of Comparative Neurology* **257**, 237–252.

SCHEMANN, M., TAMURA, K., PALMER, J. M. & WOOD, J. D. (1987). Electrical behavior of myenteric neurons in guinea-pig stomach *in vitro*. *Gastroenterology* **92**, 1618.

SCHEMANN, M. & WOOD, J. D. (1987). Neurophysiology of myenteric neurons of guinea pig stomach. *Digestive Diseases and Sciences* **32**, 925.

SCHEMANN, M. & WOOD, J. D. (1989). Synaptic behaviour of myenteric neurones in the gastric corpus of the guinea-pig. *Journal of Physiology* **417**, 519–535.

STEWARD, W. W. (1981). Lucifer dyes–highly fluorescent dyes for biological tracing. *Nature* **292**, 17–21.

WOOD, J. D. (1987*a*). Physiology of the enteric nervous system. In *Physiology of the Gastrointestinal Tract*, 2nd edn, ed. JOHNSON, L. R., pp. 367–398. New York: Raven Press.

WOOD, J. D. (1987*b*). Neurophysiological theory of intestinal motility. *Japan Journal of Smooth Muscle Research* **23**, 143–186.

WOOD, J. D. (1987*c*). Signal transduction in intestinal neurons. In *Cellular Physiology and Clinical Studies of Gastrointestinal Smooth Muscle*, ed. SZURSZEWSKI, J. H.,pp. 55–69. Amsterdam: Elsevier.

WOOD, J. D. (1989). Electrical and synaptic behavior of enteric neurons. In *Handbook of Physiology, The Gastrointestinal System Motility and Circulation*, sect. 6, vol. I, ed. WOOD, J. D., pp. 465–517. Bethesda, MD, USA: American Physiological Society.

WOOD, J. D. & MAYER, C. J. (1978). Intracellular study of electrical activity of Auerbach's plexus in guinea-pig small intestine. *Pflügers Archiv* **374**, 265–275.

ZAR, J. (1974). Biostatistical Analysis, pp. 133–151. Englewood Cliffs, NJ, USA: Prentice-Hall.